Clim Dyn (2018) 51:581–595
DOI 10.1007/s00382-017-3942-0

# The connection between the second leading mode of the winter North Pacific sea surface temperature anomalies and stratospheric sudden warming events

**Yuanpu Li[1,2] · Wenshou Tian[1] · Fei Xie[3] · Zhiping Wen[2] · Jiankai Zhang[1] · Dingzhu Hu[4] · Yuanyuan Han[1]**

Received: 20 December 2016 / Accepted: 1 October 2017 / Published online: 10 October 2017


**Abstract** Using the Hadley Center HadISST dataset and the NCEP/NCAR reanalysis dataset over the winters (December–February) from 1948 to 2014, this paper investigates the connections between the first two primary components of the sea surface temperature (SST) anomalies over the North Pacific and the stratospheric sudden warmings (SSWs) in the Northern Hemisphere winter. The results show that the winter SSW duration is more correlated to the second primary component (PC2) than the first primary component (PC1). The SSW event occurs more frequently and the winter SSW duration is longer during the positive phases of PC2 than the negative phases of PC2. The analysis also reveals that there are 10–20 year oscillations in the SSW duration after 1980, which are related to the decadal variation of PC2. The positive phases of PC2 are marked by more positive Pacific–North America (PNA) and western Pacific (WP) teleconnections in the upper troposphere. Consequently, wavenumber-1 planetary waves in the upper troposphere are strengthened and the upward Eliassen–Palm fluxes (EP fluxes) in the extratropical stratosphere are enhanced. The enhanced upward EP fluxes into the stratosphere result in SSWs persisting longer. The negative phase of PC2 has the opposite effect on the SSW duration to the positive phase of PC2. Although the SST anomalies associated with PC2 are mainly driven by the atmosphere, our model simulations show that SST anomalies of PC2 are capable of producing a feedback on the PNA and the WP and modulating the variability of SSWs.

**Keywords** Stratospheric sudden warmings · Teleconnections · Sea surface temperature

## 1 Introduction

The stratospheric sudden warming (SSW) is the most striking phenomenon in the midwinter Arctic stratosphere. During some SSW events, the temperature in the polar cap increases by more than 30 K (Butler et al. 2015). There are two kinds of SSWs in the midwinter: major and minor warmings. Major warmings are accompanied by a breakdown of the polar vortex, while minor warmings are not (Krüger et al. 2005; Butler et al. 2015). Major warmings occur at a frequency of six events per 10 years (Charlton and Polvani 2007) and minor warmings occur almost every winter (O'Neill 2003). Nevertheless, minor and major warmings have many common dynamical characteristics, and both reverse the meridional temperature gradient (Krüger et al. 2005). SSWs could have significant impacts on the winter tropospheric weather. Baldwin and Dunkerton (2001) reported that the surface pressure and storm track will be changed due to the anomalous annular mode propagating downward from the stratosphere during SSW events. Wang and Chen (2010) found that even a relatively weak warming of the polar vortex could have a significant influence on the tropospheric weather. Mitchell et al. (2013) further reported that the tropospheric weather is not only influenced

✉ Wenshou Tian
wstian@lzu.edu.cn

[1] College of Atmospheric Science, Lanzhou University, Lanzhou 730000, China

[2] Institute of Atmospheric Sciences, Fudan University, Shanghai 200433, China

[3] College of Global Change and Earth System Science, Beijing Normal University, Beijing 100875, China

[4] Key Laboratory of Meteorological Disasters of China Ministry of Education, Nanjing University of Information Science and Technology, Nanjing 210044, China

by the strength of the polar vortex, but also influenced by the shape of the polar vortex. Therefore, a better understanding of SSWs and their variations can help to improve forecasts of tropospheric weather and climate.

Pawson and Naujokat (1999) found that SSWs rarely occurred in the middle 1990s, while Charlton and Polvani (2007) noted that SSWs frequently occurred in the early 2000s. Reichler et al. (2012) further argued that the frequency of SSWs exhibited decadal variations over the past 30 years. However, whether the decadal variations of SSWs are induced by external factors or just an atmospheric internal variability remains unclear. On the other hand, most of the studies mentioned above focused mainly on major SSWs which are more restrictive than minor SSWs. Minor SSWs are also important in the stratosphere-troposphere dynamical coupling but are not well documented.

Previous studies have investigated the mechanisms responsible for the occurrence of SSWs (e.g., Holton 1976; Matsuno 1970, 1971; Quiroz 1986) and it is widely known that SSWs are induced, to a large extent, by tropospheric planetary waves propagating into the stratosphere (e.g., Matsuno 1971). The main sources of tropospheric planetary waves in the Northern Hemisphere are associated with the geographical asymmetries and the diabatic heating anomalies arising from sea surface temperature (SST) changes (Andrews et al. 1987). Particularly, the tropical SST changes associated with the El Niño-Southern Oscillation (ENSO) have significant impacts on the planetary waves and the stratospheric polar vortex (e.g., Horel and Wallace 1981; Brönnimann 2007; Garfinkel and Hartmann 2008; Bell et al. 2009; Ren et al. 2011; Zhang et al. 2015).

Many previous studies showed that the SST changes in the extratropical Pacific are mainly driven by the atmosphere. However, whether, and to what extent the SST changes over the North Pacific affect the atmosphere are still widely debated. For example, the model simulations of Kushnir et al. (2002) showed that the responses of the atmosphere to the fixed extratropical SSTs are weak and unstable. Nevertheless, Hu and Pan (2009) and Jadin et al. (2010) and Hu et al. (2014) reported that the tropospheric planetary waves propagating upward into the stratosphere are modulated by the SST anomalies over the North Pacific. Some other studies found that the ocean–atmosphere interactions related to the western boundary currents (WBC), extending from the tropics to the extratropical area, play a key role in the decadal variability of the extratropical atmosphere in several coupled climate models (Pierce et al. 2001; Wu and Liu 2005; Kwon and Deser 2007). Hurwitz et al. (2011) found that the anomalous cold stratospheric polar vortex in March 2011 was caused by the SST anomalies over the North Pacific rather than the ENSO or the quasi-biennial oscillation (QBO). Hurwitz et al. (2012) further showed that the negative SST anomalies over the North Pacific often intensify the Aleutian Low and the Western Pacific (WP) teleconnection pattern, which may affect the stratospheric polar vortex (Wallace and Gutzler 1981; Nishii et al. 2010).

Generally, there are two distinct modes in the North Pacific SST variations: one is the Pacific Decadal Oscillation (PDO), which is typically defined as the first leading mode of the North Pacific SST anomalies by the empirical orthogonal function (EOF) analysis (Mantua et al. 1997); the other is the second leading mode of the North Pacific SST anomalies (Nakamura et al. 1997; Bond et al. 2003), also known as the "Victoria mode" (Ding et al. 2015). This mode is also closely connected to the North Pacific Gyre Oscillation (NPGO; Di Lorenzo et al. 2008). The influence of the first mode of the North Pacific SST anomalies on the stratospheric polar vortex has been studied using reanalysis data (Jadin et al. 2010; Woo et al. 2015) and model simulations (Kren et al. 2016). All of these studies found that the polar stratosphere tends to be warmer during the positive phases of the PDO. However, the linkages between the second leading mode of the North Pacific SST anomalies and SSW variations at interannual and decadal time scales have not been investigated in detail thus far.

In this paper, the interannual and decadal variations in SSWs are investigated from the perspectives of duration and frequency. To understand how the SST changes over the Pacific modulate SSWs, the different modes of the North Pacific SST anomalies and the changes of the geopotential height and planetary waves in the upper troposphere and stratosphere are analyzed. The remainder of the paper is arranged as follows: Sect. 2 presents the datasets and methods employed. The variations in SSWs and Pacific SST anomalies are described in Sect. 3. Section 4 analyzes the connection between the North Pacific SST anomalies and the planetary waves in the troposphere and stratosphere. The conclusions and discussions are given in Sect. 5.

## 2 Datasets and methods

The variations in the winter North Pacific SST anomalies are explored using the Hadley Center HadISST dataset (Rayner et al. 2003), which has a 1° by 1° horizontal resolution and covers the winters from 1948 to 2014 (hereafter, "winter" refers to December, January and February, including 201 months). In this study, the North Pacific is defined as the region from 10°N–65°N and 100°E–100°W. The climatological monthly mean SST is removed from the raw data to obtain the anomalies of SST. The SST anomalies in December, January, and February have been detrended over the 67 years to capture the interannual anomalies. The EOF analysis of the SST anomalies results in two leading modes (shown in Fig. 1) and their principal components. The first two principal components are averaged over the winter to

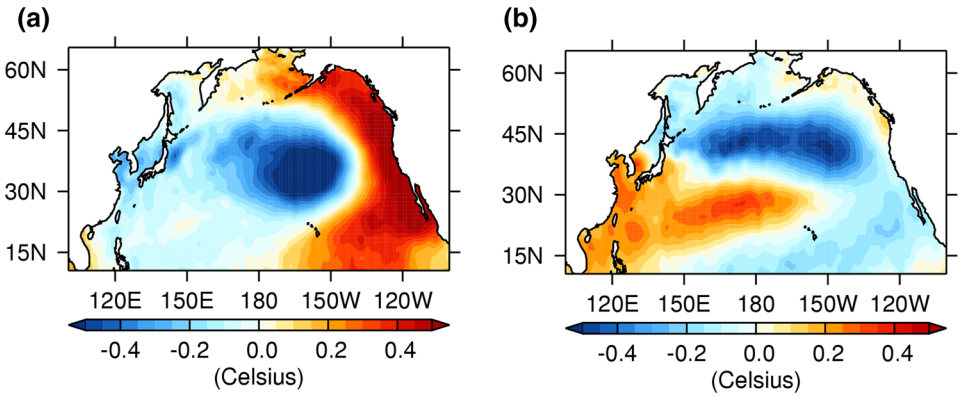


**Fig. 1** Regression maps of SST anomalies (unit: °C) onto the **a** first and **b** second principal components (PC1, PC2) of winter North Pacific SST anomalies based on the HadISST dataset

get the winter mean time series (hereafter PC1 and PC2 for short, shown in Fig. 2b, c). The winter tropical Pacific SST variations are represented by the Nino 3 index, which is defined as the averaged detrended SST anomalies over the Nino 3 region (5°N–5°S and 150°W–90°W).

The meteorological data analyzed in this work is the NCEP/NCAR reanalysis dataset, which has a 2.5° by 2.5° horizontal resolution covering the winters from 1948 to 2014, provided by the National Center for Environmental Prediction and National Center for Atmospheric Research. The duration and frequency of SSWs are derived from the meridional temperature gradient between 60°N and 90°N at 10 hPa and the zonal mean zonal wind at 60°N and at 10 hPa. A SSW event occurs when the meridional temperature gradient reverses from negative to positive. In this approach, SSWs include both major and minor warmings. A major SSW event further requires that the zonal mean zonal wind at 10 hPa and at 60°N reverses to easterly; otherwise it is defined as a minor warming. The duration of SSWs, including both major and minor SSWs, can

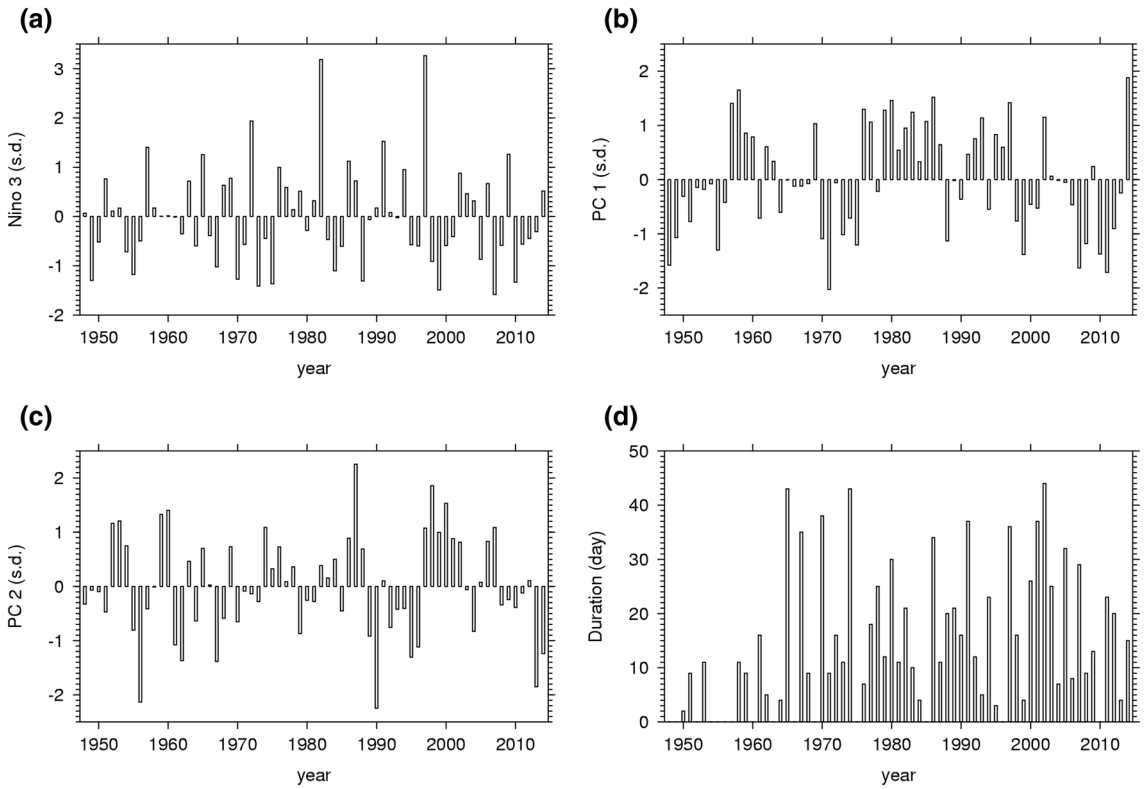


**Fig. 2** Time series of the standardized **a** Nino 3 Index, **b** PC 1 index and **c** PC 2 index derived from the HadISST dataset. **d** The time series of duration (unit: day) of SSWs defined by the meridional temperature gradient derived from the NCEP/NCAR dataset over the winters of 1948–2014

be measured by the number of days when the meridional temperature gradient between 60°N and 90°N at 10 hPa is positive. The duration of major SSWs can be measured by the number of days when the zonal mean zonal wind at 60°N at 10 hPa is easterly. The method for determining the frequency of SSWs can also be found in Charlton and Polvani (2007). In this study, two separated SSW events must be more than 20 days apart in order to exclude SSWs which are in close proximity to each other.

The Pacific–North America (PNA) and western Pacific (WP) teleconnections are defined by the EOF analysis of the geopotential height anomalies in the Northern Hemisphere (180°W–180°E, 0°–90°N) at 200 hPa. The geopotential height anomalies in December, January, and February are detrended over the 67 years. The second EOF mode is the PNA pattern and the third mode is the WP pattern. Monthly and daily geopotential height anomalies are projected onto the PNA and the WP patterns to derive the monthly and daily teleconnection indices.

To extract the wavenumber-1 and wavenumber-2 components of planetary waves, a Fourier decomposition of the geopotential height anomalies is utilized in the zonal direction. To identify planetary wave fluxes in the atmosphere, Eliassen–Palm fluxes (EP fluxes) are employed and are calculated using the formula given by Andrews et al. (1987).

Composite analyses of the meteorological variables are performed depend on different phases of PC2. The thresholds of the positive and negative phases of PC2 are +0.5 and −0.5 standard deviation (sdv) except otherwise stated. There are 21 positive PC2 winters including 1952, 1953, 1954, 1959, 1960, 1965, 1969, 1974, 1976, 1984, 1986, 1987, 1988, 1997, 1998, 1999, 2000, 2001, 2002, 2006 and 2007, and 17 negative PC2 winters including 1955, 1956, 1961, 1962, 1964, 1967, 1968, 1970, 1979, 1989, 1990, 1992, 1995, 1996, 2004, 2013 and 2014.

The relationship of two time series is estimated using Pearson correlation coefficient. The statistical significance of correlation coefficient is tested by the two-tailed Student's *t*-test employing the effective number of degrees of freedom ($N^{\text{eff}}$) (Bretherton et al. 1999). The approximation of $N^{\text{eff}}$ is defined as the following (Li et al. 2012):

$$\frac{1}{N^{eff}} \approx \frac{1}{N} + \frac{2}{N}\sum_{j=1}^{N}\frac{N-j}{N}\rho_{XX}(j)\rho_{YY}(j) \quad (1)$$

where $N$ denotes the sample size. $\rho_{XX}$ and $\rho_{YY}$ denote the autocorrelation coefficients of two time series at time lag $j$. All correlation coefficients given in the paper are significant above the 95% confident level unless otherwise stated.

The two-tailed Kolmogorov–Smirnov (KS) test is used to examine whether the probability distribution functions (PDFs) of two samples are significantly different from each other, and the corresponding results shown in the following analyses are significant above the 99% confidence level unless otherwise stated.

The results derived from the reanalysis data are further verified by the third version of the Whole Atmosphere Community Climate Model (WACCM3), which has been shown to have a good performance in simulating SSW events (Taguchi and Hartmann 2006). The details of the model are documented in Garcia et al. (2007). Two time-slice simulations with a horizontal resolution of 1.9° by 2.5° were performed in this study. In run E1, the forcing SST field is constructed by adding the Pacific SST anomalies (10°N–65°N and 100°E–100°W) corresponding to 1 sdv of PC2 time series to the climatological SST field. In run E2, the forcing SST field is constructed by subtracting the Pacific SST anomalies (10°N–65°N and 100°E–100°W) corresponding to 1 sdv of PC2 time series from the climatological SST field. All simulations have been run for 34 years and the model output of the first 4 years accounting for the model spin-up are excluded.

## 3 The relations of the variations in the North Pacific SST and SSWs

The winter variations of the tropical Pacific SST are represented by the time series of the Nino 3 index in Fig. 2a. The winter variations in the extratropical Pacific SST anomalies are represented by the time series of PC1 and PC2 in Fig. 2b, c, respectively. The corresponding spatial patterns of PC1 and PC2 are shown in Fig. 1a, b, respectively. The first mode derived from the winter North Pacific SST anomalies exhibits a west-east dipole pattern; i.e., one center appears within the domain of 30°N–45°N, 180°–150°W, and the other center appears along the coast of the North American continent. The spatial pattern of PC1 is similar to that of the PDO given by Mantua and Hare (2002). The correlation coefficient between the PDO index (downloaded from http://jisao.washington.edu/pdo/) and PC1 is 0.9. The second mode derived from the winter North Pacific SST anomalies has a north–south dipole structure, which is consistent with the results given by Bond et al. (2003) and Furtado et al. (2011). This structure is also similar to the SST anomalies regressed onto the NPGO index (http://www.o3d.org/npgo/npgo.php). The PC2 is correlated with the NPGO index with a correlation coefficient of 0.7. We can see from Fig. 1b that there are positive SST anomalies oriented from northeast to southwest within the domain of 10°N–30°N, 110°E–150°W when PC2 is in its positive phase. These positive SST anomalies belong to Pacific western boundary current, which starts from Luzon Island, through East China Sea, to the central Pacific.

Figure 2d shows the long-term variations in the SSW duration defined by the temperature gradient over the winters of 1948–2014. The correlation analyses are applied to the SSW duration and the three indices presenting Pacific SST variabilities. Before the analyses, the linear trends in the time series are removed. The correlation coefficients between the SSW duration and the Nino 3, PC1, PC2 are 0.24, 0.04 and 0.22, respectively. The correlation between the SSW duration and PC1 are not statistically significant. The impact of the tropical SST changes associated with the ENSO on SSWs in the Northern Hemisphere has been reported in previous studies. For examples, the model simulations by Taguchi and Hartmann (2006) showed that the frequency of SSWs in the Northern Hemisphere during El Niño winters is twice more than that during La Niña winters. Some studies showed that the polar vortex in the Northern Hemisphere tends to be warmer during the El Niño winters than the La Niña winters (Brönnimann 2007; Bell et al. 2009; Calvo et al. 2010). It is notable that the correlation coefficient between the SSW duration and PC2 is comparable to that between the SSW duration and the Nino 3 index. At the same time, the correlation coefficient between PC2 and the Nino 3 index is 0.1 and it does not pass the significance test. The result here implies that apart from the SST anomalies associated with the Nino 3 index, the SST anomalies associated with PC2 have a close relation with the SSW duration.

It is also notable that the correlation coefficient between the SSW duration and PC2 is much higher than that between the SSW duration and PC1, although PC1 is the first mode accounting for the majority of the North Pacific SST variabilities. Figure 3 shows the means of the duration and the frequency of SSWs defined by the meridional temperature gradient when PC1 and PC2 are in different phases for the winters of 1948–2014. We can see from Fig. 3a, c that the warming events occur more frequently and the warming duration is longer during the positive phases of PC1 ($>1$ sdv) than the negative phases of PC1 ($<-1$ sdv). The frequency of SSWs during the positive phases of PC1 is 1.7 times more than that during the negative phases of PC1. The frequency ratio of the weak stratospheric vortex events between different phases of the PDO is 1.3 (Woo et al. 2015), which is comparable to the result here. However, we find that the results highly depend on the threshold for defining different phases of PC1; i.e., if the $\pm$PC1 phases are chosen based on $\pm 0.5$ sdv of the time series, the differences in the duration and the frequency between $\pm$PC1 phases are insignificant, which is consistent with the low

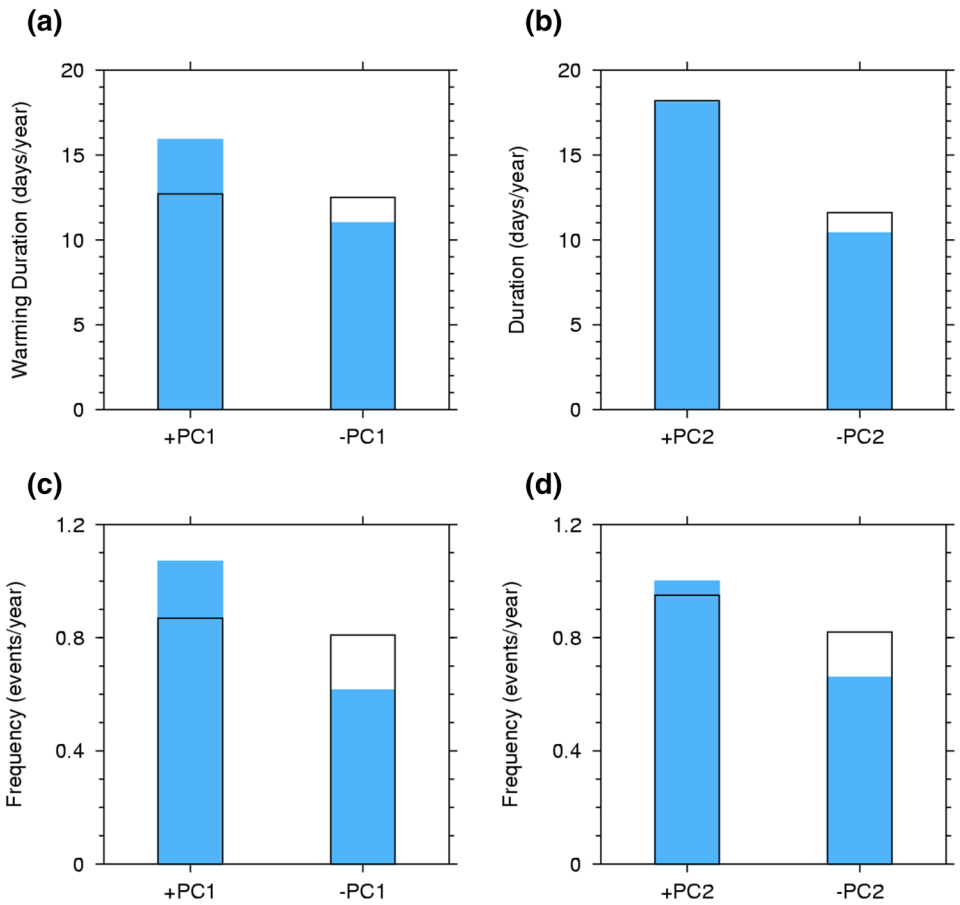


**Fig. 3** The means of **a, b** the duration (unit: days/year) and **c, d** the frequency (unit: events/year) of SSW events defined by the meridional temperature gradient during different phases of **a, c** PC1 and **b, d** PC2 derived from the NCEP/NCAR dataset from 1948 to 2014. The blue bars and black boxes represent the results using $\pm 1$ and $\pm 0.5$ sdv as the thresholds for different phases, respectively

correlation coefficient between PC1 and the SSW duration. The model result in Kren et al. (2016) also indicated that the responses of SSWs to different phases of the PDO are statistically indifferent. The result here may imply that the responses of SSWs to the PDO are significant only when the PDO index is strongly positive or negative. Figure 3b, d indicate that SSWs defined by the temperature gradient occur approximately 1.5 times more frequently during the positive phases of PC2 than the negative phases of PC2. The duration of SSWs during the positive phases of PC2 is almost twice as long as that during the negative phases of PC2. This results are robust when $\pm 1$ sdv are chosen to determine different phases of PC2.

Figure 4 shows the winter mean duration and frequency of SSWs defined by the zonal mean zonal wind at 60°N at 10 hPa when PC1 and PC2 are in different phases from 1948 to 2014. It can be seen that the duration and the frequency of SSWs are significantly extended and increased during the positive phases of PC2 than the negative phases of PC2. The differences in the duration and the frequency of SSWs between different PC1 phases is statistically insignificant. From Figs. 3 and 4, we can see that the positive phases of PC2 are accompanied with more SSW events and longer SSW duration regardless of how the SSWs are defined, either by the meridional temperature gradient or by the zonal mean zonal wind at 10 hPa. Hurwitz et al. (2012) investigated the effects of the high and low North Pacific SSTs on the northern polar stratosphere and they found that the number of winters which have SSWs was three times more under the low North Pacific SST condition than the high North Pacific SST condition. This ratio is close to the ratio derived from SSW frequency defined by the zonal mean zonal wind at 10 hPa, but higher than the ratio derived from SSW frequency defined by the meridional temperature gradient at 10 hPa. To separate the impact of the ENSO on the SSWs, Fig. 5 further shows the mean duration and frequency of SSWs during different phases of PC2, but excluding the El Niño and La Niña years. A winter is considered as El Niño if the winter mean Nino 3 index is above 1K; a winter is considered as La Niña winter if the winter mean Nino 3 index under $-1$K. Figure 5 reveals that if the El Niño and the La Niña years are removed from the statistical sample; the frequency and the duration of SSWs are still significantly more and longer during the positive phases of PC2 than the negative phases of PC2.

Figure 6 shows the wavelet analyses of the time series of PC1 and PC2 as well as the time series of the Nino 3 index and the SSW duration defined by the meridional temperature

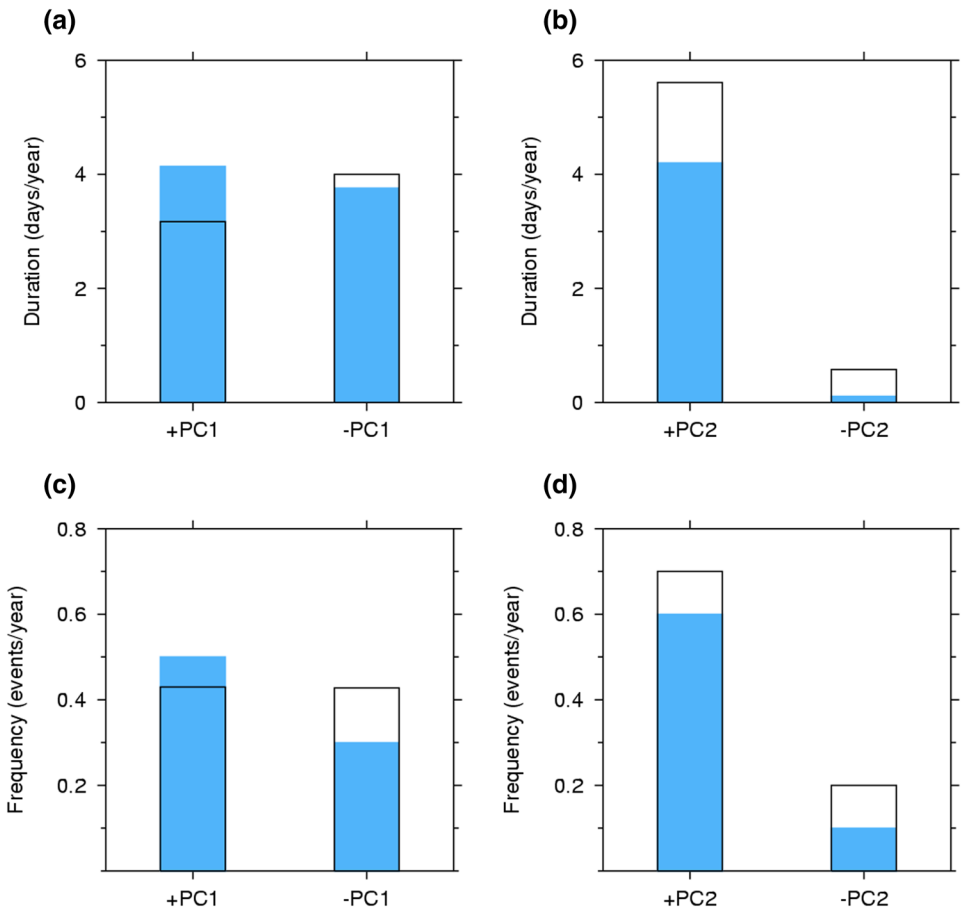


**Fig. 4** The means of **a, b** the duration (unit: days/year) and **c, d** the frequency (unit: events/year) of SSW events defined by the zonal mean zonal wind during different phases of **a, c** PC1 and **b, d** PC2 derived from the NCEP/NCAR dataset from 1948 to 2014. The blue bars and black boxes represent the results using $\pm 1$ and $\pm 0.5$ sdv as the thresholds for different phases, respectively

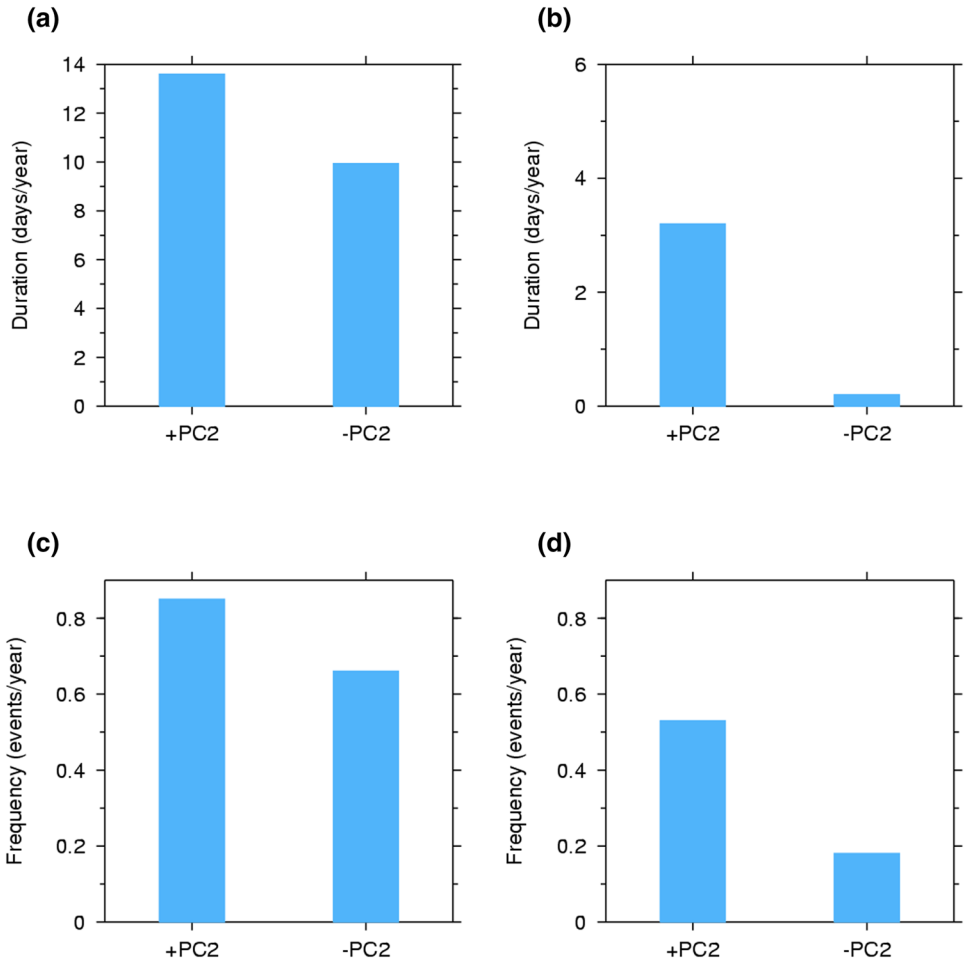


**Fig. 5** The means of **a, b** the duration (unit: days/year) and **c, d** the frequency (unit: events/year) of SSW events defined by **a, c** the temperature gradient and **b, d** the zonal mean zonal wind during different phases of PC2 excluding El Niño and La Niña years. The results use ± 0.5 sdv as the thresholds for different phases of PC2. If the Nino 3 index above 1K then it is considered as El Niño winter; if the Nino 3 index under − 1 K then it is considered as La Niña winter

gradient at 10 hPa. We can see from Fig. 6 that the Nino 3 index has an oscillation with a period of 3–7 years and PC1 has an oscillation with a period of more than 20 years, as has also been reported in earlier studies (e.g., Newman et al. 2003). After 1975, PC2 has an oscillation with a period of 10–20 years. After applying 10-year running mean to PC2 time series, we found that on the decadal scale, PC2 experienced negative phases in 1958–1972 and 1988–1995 and experienced positive phases in 1973–1987 and 1996–2007. The SSW duration has an oscillation with a period of 3–7 years for 1960–1978 and 1985–2010 and an oscillation with a period of 10–20 years after 1980. The signal in SSW duration with a period of 3–7 years is in accordance with the period of the Nino 3 index, while the signal in SSW duration with a period of 10–20 years after 1980 is possibly connected with PC2. The average durations of SSWs defined by the meridional temperature gradient at 10 hPa are 13.8 and 18.5 days per year in the negative phases of PC2 and in the positive phases of PC2, respectively. The average durations of SSWs defined by the zonal mean zonal wind at 10 hPa are 2.3 and 5.8 days per year in the negative phases of PC2 and in the positive phases of PC2, respectively. The above results further confirm that the SSW duration is connected to PC2 on decadal timescales.

## 4 The changes in planetary waves related to PC2

Previous studies have provided convincing evidence that the activity of SSWs is directly influenced by tropospheric waves propagating upward into the stratosphere, particularly the wavenumber-1 and wavenumber-2 tropospheric waves (Martius et al. 2009; Woollings et al. 2010; Waugh and Polvani 2010). Figure 7a shows the composited 200 hPa geopotential height (GH) anomalies during the positive phases of PC2. There are negative GH anomalies over the Aleutian Islands and positive GH anomalies over the western subtropical Pacific and Northern Canada. The GH anomalies during the negative phases of PC2 are presented in Fig. 7b. The spatial pattern of the negative phases of PC2 is almost opposite to the pattern of the positive phases of PC2.

Li and Tian (2017) found that before the occurrence of SSWs which last relatively longer, there are more positive phases of PNA and WP teleconnections. They also showed

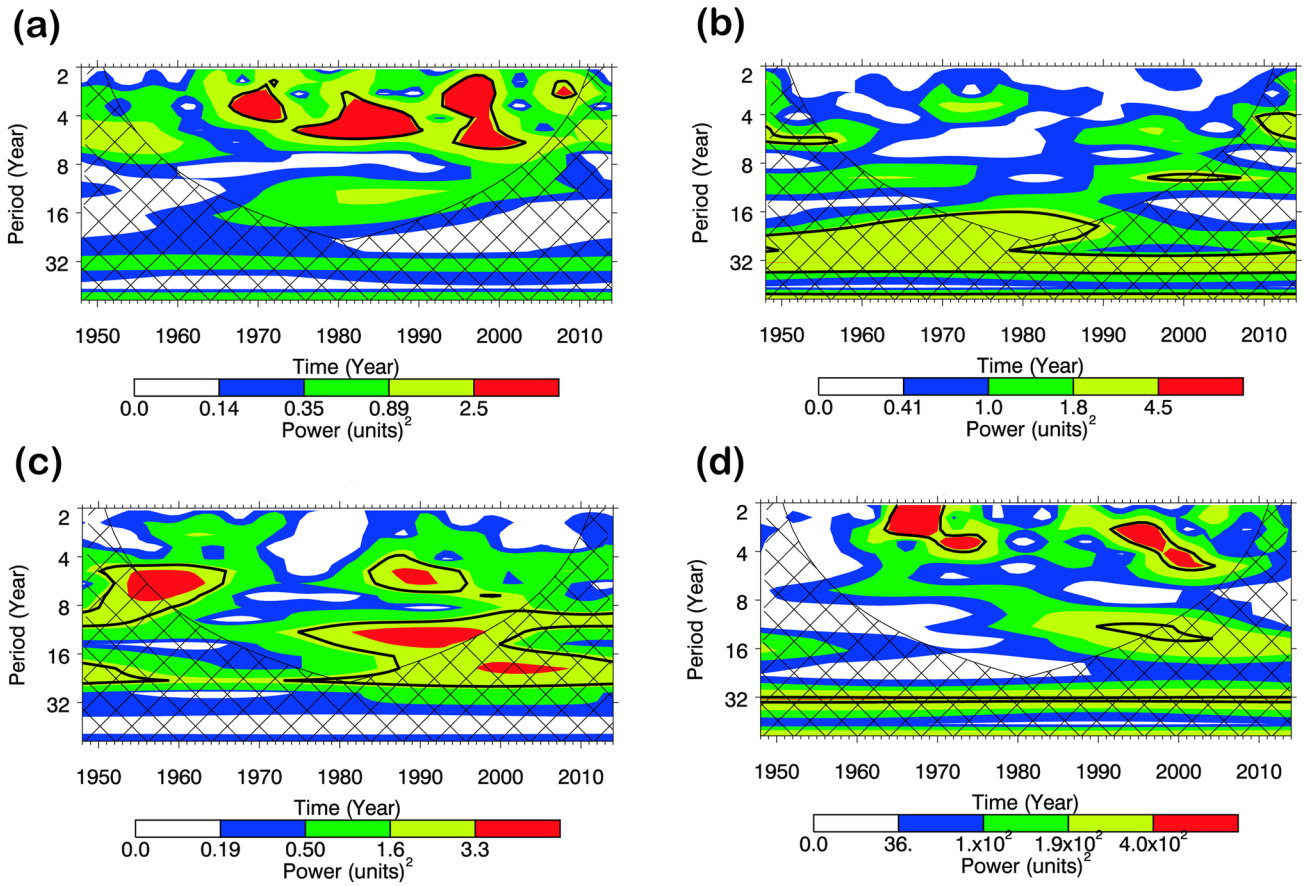


**Fig. 6** The wavelet power spectrum of **a** the Nino 3 index, **b** PC1, **c** PC2 and **d** the warming duration defined by the meridional temperature gradient. The contour levels are chosen so that 75, 50, 25, and 5% of the wavelet power is above each level, respectively. The cone of influence is represented by the cross-hatched region. Black contours show the 90% significance level using a white-noise background spectrum

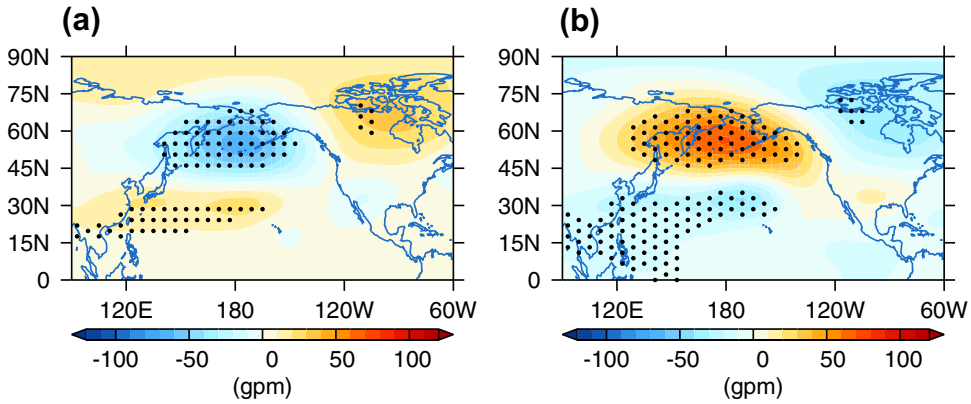


**Fig. 7** The composited 200 hPa geopotential height (unit: gpm) anomalies during **a** the positive and **b** the negative phases of PC2 derived from the NCEP/NCAR dataset in the period from 1948 to 2014. The anomalies over dotted regions are statistically significant at the 95% confidence level according to Student's t-test

that the combination of the positive phases of PNA and WP is accompanied by the strengthening of wavenumber-1 waves and vice versa. Therefore, it is necessary to examine the connections between PC2 and teleconnections. Figure 8 shows the regression maps of GH at 200 hPa in the winter onto the WP and PNA indices as well as the probability density functions (PDFs) of WP and PNA daily indices during different phases of PC2 derived from the NCEP/NCAR dataset from 1948 to 2014. Note that the spatial structures of GH anomalies during different phases of PC2 have a good resemblance with the spatial structures of WP and PNA given in Fig. 8a, b. From Fig. 8c, d, we can see that

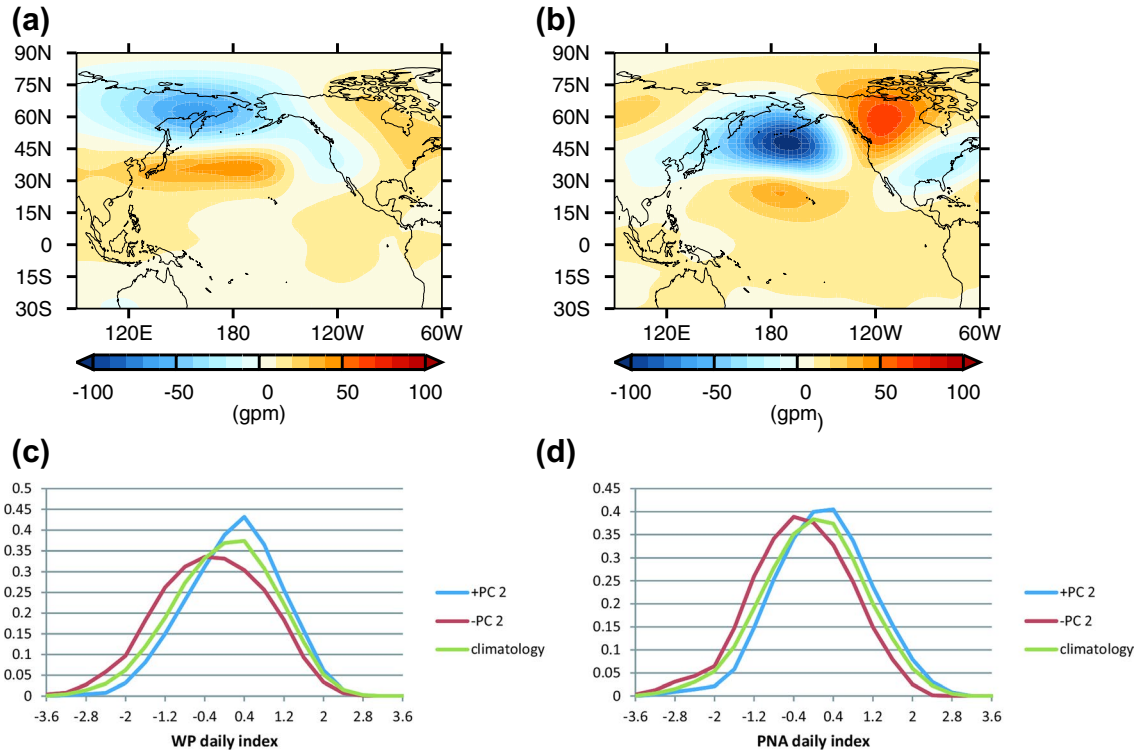


**Fig. 8** The regression maps of geopotential height at 200 hPa (unit: gpm) with the **a** WP index and **b** PNA index in the winter. The PDF of the **c** WP and **d** PNA daily indices during the positive and negative phases of PC2 derived from the NCEP/NCAR dataset from 1948 to 2014

during the positive phases of PC2, the probability for positive WP and PNA teleconnections to occur is higher. This conclusion derived from Fig. 8c, d is still valid if the teleconnection indices defined by Wallace and Gutzler (1981) are used (not shown). The correlation coefficient between PC2 and the winter mean WP is 0.37 and the correlation coefficient between PC2 and the winter mean PNA is 0.44, implying close linkages between PC2 and the WP and PNA teleconnections.

To further understand the changes of the planetary waves in the upper troposphere during different phases of PC2, Fig. 9 shows the wavenumber-1 and wavenumber-2 components of the 200 hPa GH anomalies composited with respect to different phases of PC2. During the positive phases of PC2, the negative anomalous center of the wavenumber-1 component is located between Northeast Asia and the Northeast Pacific, and the positive anomalous center is located within the domain from Northeast Canada to Eastern Europe (Fig. 9a). The wavenumber-1 anomalies coincide with the climatological pattern of wavenumber-1, implying the wavenumber-1 component in the upper troposphere is enhanced. During the positive phases of PC2, the two negative anomalous centers of wavenumber-2 component appear over the Northwest Pacific and the North Atlantic while the two positive anomalous centers are located over Canada and Siberia (Fig. 9b). The amplitudes of the wavenumber-2 anomalies are comparable to the wavenumber-1 anomalies. However, the wavenumber-2 anomalies are nearly 90° out of phase with the climatological pattern; i.e., some areas of the wavenumber-2 anomalies coincide with the climatology while other areas of the anomalies are contrary to the climatology. Thus, changes in the strength of wavenumber-2 component are not as obvious as the changes in wavenumber-1 component, implying that the wavenumber-2 waves may play a less important role in the planetary wave changes. The magnitudes of wavenumber-1 and wavenumber-2 anomalies during the negative phases of PC2 are similar to those during the positive phases of PC2 but the signs of the anomalies are opposite, implying that the wavenumber-1 component in the extratropical upper troposphere is weakened.

Figure 10a, b further illustrate the changes in the strength of the planetary waves in the extratropical upper troposphere associated with PC2. The strength of planetary waves is measured by the vertical component of EP fluxes ($F^{(z)}$) over the latitude band 40°N–90°N. The strength of wavenumber-1 component in the extratropical upper troposphere is enhanced during the positive phases of PC2 and depressed during the negative phases of PC2. The strength of wavenumber-2 component in the extratropical upper troposphere does not change much during the positive phases of PC2 due to the reason explained in Fig. 9. The strength of wavenumber-2 component at middle latitudes in the upper troposphere

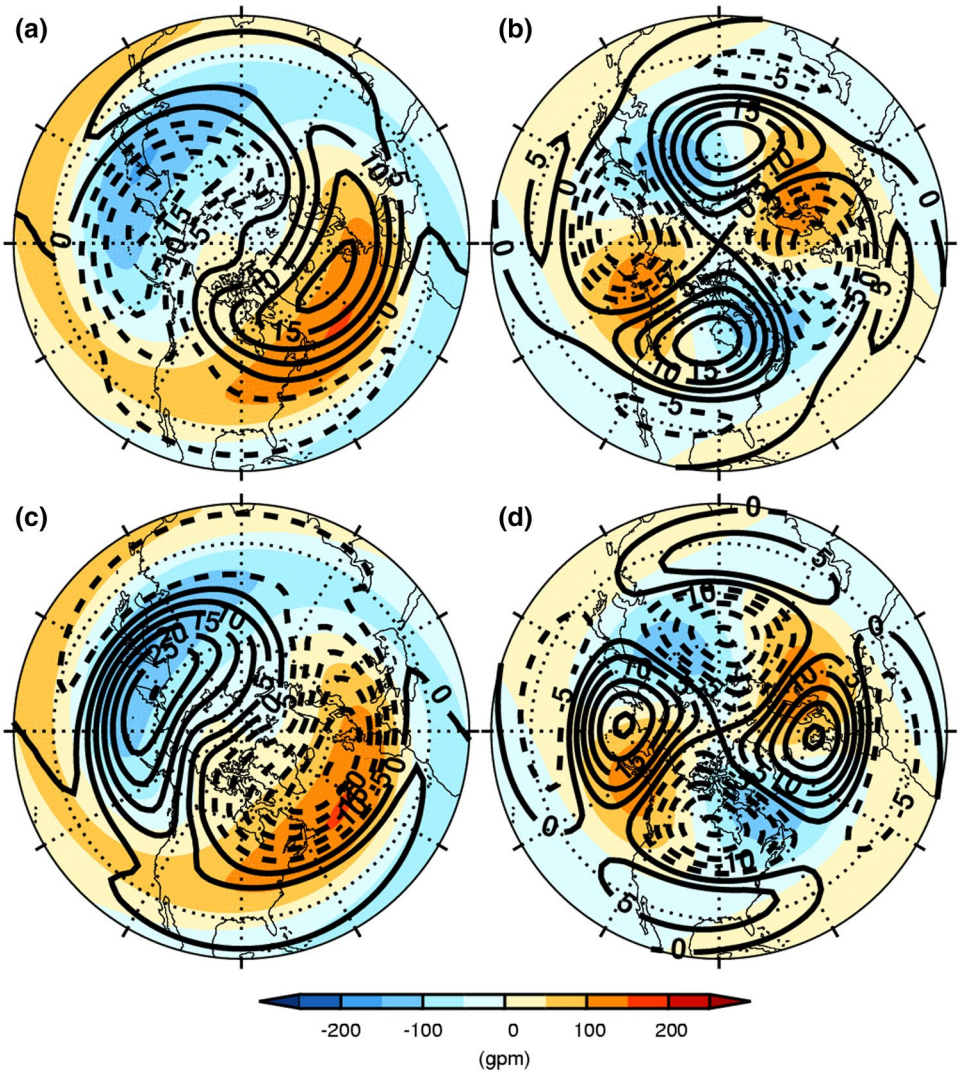


**Fig. 9** Composited **a, c** wavenumber-1 and **b, d** wavenumber-2 components of the geopotential height anomalies at 200 hPa (black contour lines with the intervals of ± 5, ± 10, ± 15 gpm) during **a, b** the positive phases and **c, d** the negative phases of PC2 derived from the NCEP reanalysis dataset from 1948 to 2014. The color-filled contours show climatological distributions

is increased during the negative phases of PC2 but the magnitude of the change of wavenumber-2 component is relatively small compared to that of wavenumber-1 component. Figure 10c, d show the time series of the strength of wavenumber-1 and -2 components in the northern extratropical upper troposphere. The correlation coefficient between PC2 and the strength of wavenumber-1 component is 0.5. The correlation coefficient between PC2 and the strength of wavenumber-2 component is − 0.3. Meanwhile, the averaged strength of wavenumber-1 component in the extratropical upper troposphere is approximately 1.6 times as large as that of wavenumber-2 component, suggesting that the wavenumber-1 component dominates the variabilities of the planetary waves in the extratropical upper troposphere. The correlation coefficient between wavenumber-1 component and the SSW duration defined by the meridional temperature gradient at 10 hPa is 0.4, while the correlation coefficient between wavenumber-2 component and the SSW duration is − 0.2, but statistically insignificant.

To understand how the planetary waves above the upper troposphere would change during different phases of PC2, Fig. 11 shows the EP flux vectors and EP flux divergence differences between different phases of PC2. Figure 11a shows that there are more upward planetary wave fluxes during the positive phases of PC2 than the negative phases of PC2, accompanied by more negative anomalies in the EP flux divergence in the stratosphere. The differences in wavenumber-1 fluxes given by Fig. 11b are consistent with Fig. 11a. Figure 11c shows that there are less upward wavenumber-2 EP fluxes during the positive phases of PC2 than the negative phases of PC2, accompanied by more positive anomalies in EP flux divergence in the stratosphere. The changes of wavenumber-2 fluxes are overwhelmed by the much larger changes of wavenumber-1 fluxes. The results here suggest that the positive (negative) phases of PC2 correspond to stronger (weaker) upward wave fluxes and negative (positive) EP flux divergence anomalies in the stratosphere, which would drive the polar vortex warmer (cooler); i.e., minor

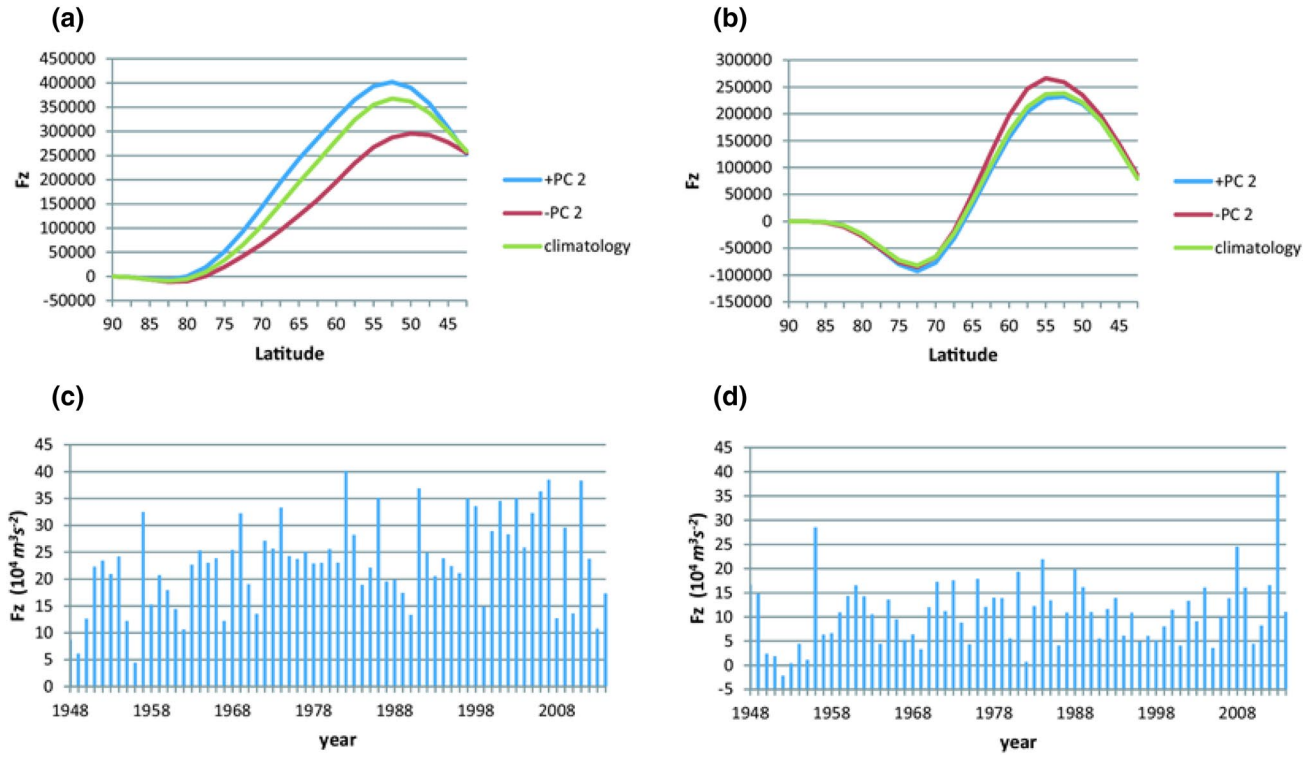


**Fig. 10** Vertical component of EP fluxes ($F^{(z)}$) at 200 hPa (divided by the air density, unit: $m^3s^{-2}$) associated with **a** wavenumber-1 and **b** wavenumber-2 during different phases of PC2. The time series of the $F^{(z)}$ (unit: $10^4$ $m^3s^{-2}$) at 200 hPa averaged over the latitude band 45°N–90°N associated with **c** wavenumber-1 and **d** wavenumber-2 components derived from the NCEP/NCAR reanalysis data over the winters of 1948–2014

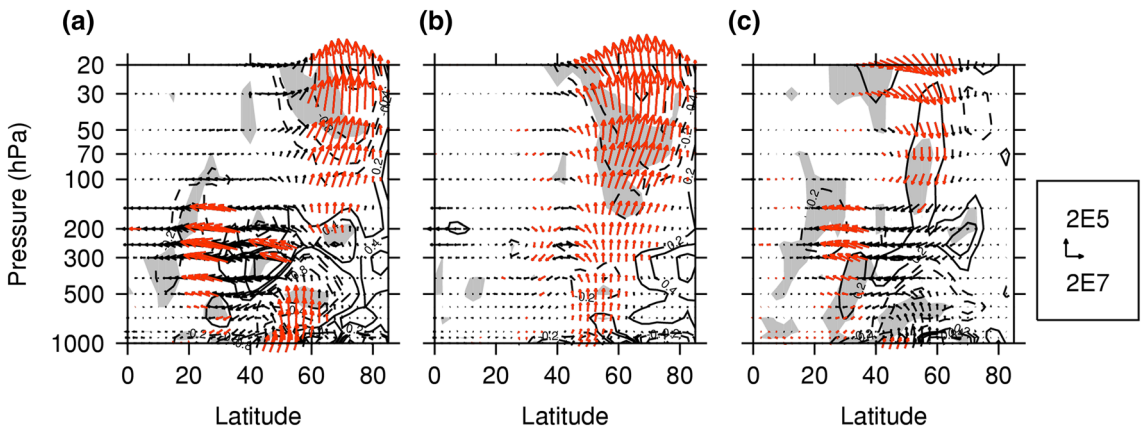


**Fig. 11** **a** Differences in the EP fluxes (unit: $m^3s^{-2}$) and EP flux divergence (unit: $10^{-5}$ $ms^{-2}$) and **b** the wavenumber-1 component and **c** wavenumber-2 component between positive and negative phases of PC2 derived from the NCEP/NCAR dataset from 1948 to 2014. The EP flux vectors of $(F^{(\phi)}, F^{(z)})/\rho$ are scaled by the ratio between the vertical and horizontal distances on the plot. The EP fluxes are plotted in red if the differences in the vertical components are significant at the 95% confidence level. The differences in EP flux divergence are shaded in gray if the differences are statistically significant at the 95% confidence level according to Student's t-test

SSWs are more likely to occur when PC2 is in the positive phase.

Chhak et al. (2009) found that the NPGO, which is related to PC2, is induced by the North Pacific Oscillation and the WP teleconnection. Although the extratropical SST changes in the Northern Hemisphere are mainly driven by the surface winds, the extratropical atmosphere is also impacted by the ocean at the same time (e.g., Nigam 2003). Using a climate

model, Hurwitz et al. (2012) verified that the North Pacific SST anomalies have a significant effect of on the Northern Hemispheric winter atmosphere. Thus, the third version of the Whole Atmosphere Community Climate Model (WACCM3) is used to verify the results derived from the reanalysis data. Two time-slice simulations were performed in this study. The run E1 simulated the atmosphere during the positive phases of PC2 by adding the Pacific SST anomalies (10°N–65°N and 100°E–100°W) corresponding to 1 sdv PC2 to the climatological SST field. The run E2 simulated the atmosphere during the negative phases of PC2 by subtracting the Pacific SST anomalies corresponding to 1 sdv PC2 from the climatological SST field. Figure 12 shows the differences in the zonal mean zonal wind between different phases of PC2 derived from the reanalysis data and the model simulations. We can see that the model is able to capture the changes of the polar vortex during different phases of PC2. Both in the reanalysis data and in the model simulation, the polar vortex is significantly weakened during the positive phases of PC2. However, the differences of the zonal mean zonal wind in the northern polar stratosphere in the model data are smaller in magnitude than those in the reanalysis data. The SSW duration defined by the zonal mean zonal wind at 10 hPa is 1 day/year and 0.2 day/year during E1 and E2, respectively. The SSW duration defined by the meridional temperature gradient is 14.9 and 13.2 day/year during E1 and E2. The model is able to simulate the differences of the SSW duration between different phases of PC2, but the differences in the model data are smaller than those in the reanalysis data. The model results here confirm that the SST anomalies of PC2 partly account for the difference in the SSW duration between different phases of PC2.

Here we use model results to surmise a possible mechanism to explain how SST anomalies of PC2 produce a feedback on the PNA and the WP. Figure 13a shows the simulated differences of the winter mean Outgoing Longwave Radiation (OLR) between E1 and E2. We can see that the OLR over the western subtropical Pacific (10°N–30°N 120°E–160°E) is lower during the positive phases of PC2 than the negative phases of PC2, which implies the convective activity over this region is more active during the positive phases of PC2 than the negatives phase of PC2. The differences in OLR are induced by the SST differences since only SSTs are different between E1 and E2. The changes of the convective activity over the western subtropical Pacific would modulate the precipitation and the latent heat released by the precipitation, which would modulate the GH field. Figure 13b shows the differences in 200 hPa GH between runs E1 and E2. There are positive GH differences over the southern China and the subtropical Pacific and the polar

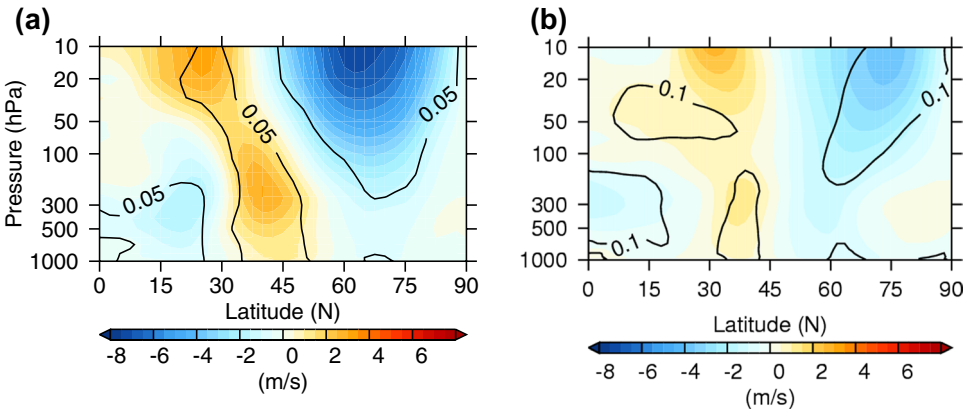


**Fig. 12** The winter differences of zonal mean zonal wind (unit: m/s) between different phases of PC2 derived from **a** reanalysis data and **b** model simulation data. The differences in the black lines in **a** and **b** are statistically significant above 95% and 90% confidence level according to the Student's t-test

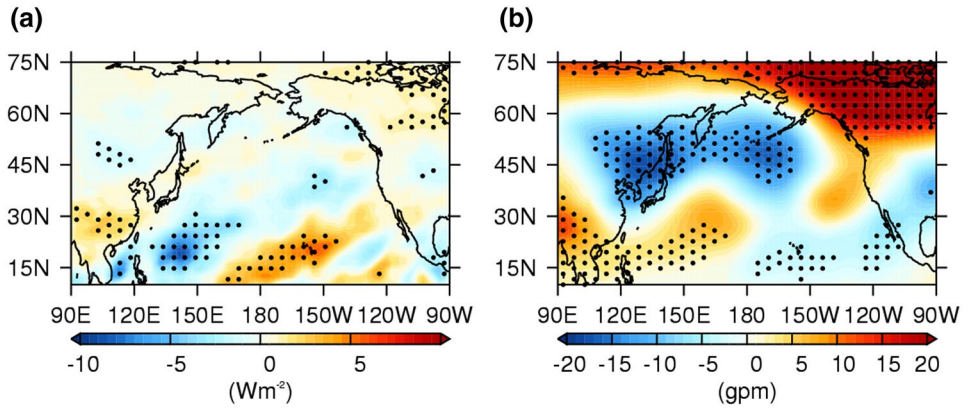


**Fig. 13** **a** OLR (unit: $Wm^{-2}$) and **b** 192.5 hPa geopotential height differences (unit: gpm) over the Pacific region between runs E1 and E2. The differences over dotted regions are statistically significant above 99% confidence level according to the Student's t-test

region. There are negative GH differences at middle and high latitudes. The pattern of the GH differences derived from the model simulations is similar to the reanalysis data, but the magnitude of GH differences derived from the model simulations is smaller than the reanalysis data. The convective anomalies induced by the SSTs of PC2 could modulate the tropical and subtropical GH via the latent heat release and the tropical and subtropical GH would further affect the extratropical GH via the PNA and WP. There are still some issues worth further investigation, e.g., this model study used climatological SSTs, thus the feedback from the PNA and the WP onto the ocean has not been seen. It is also possible that other processes associated with PC2 can modulate the tropospheric GH and then insert an impact on the SSW duration.

## 5 Conclusions and discussion

The variations of SSWs in the Northern Hemisphere are investigated in this study from the perspectives of duration and frequency using the NCEP/NCAR reanalysis datasets. We found that there were interannual and decadal variations in the SSW duration during the period of 1948–2014. The interannual variation in the SSW duration is related to the ENSO and PC2. An oscillation in the SSW duration with a period of 10–20 years is detected in the time series after 1980, which is consistent with the oscillation in the wavelet spectrum of PC2, implying that there is a connection between PC2 and the decadal variations in the SSW duration.

We found the SSW duration and the SSW frequency are more related to PC2 than PC1. During the positive phases of PC2, the Aleutian Low and the Subtropical High are strengthened. There are more positive WP and PNA teleconnections in the extratropical troposphere. The strengthened wavenumber-1 waves in the troposphere increase the upward wave fluxes into the stratosphere, which lead to more SSWs occur.

Although the extratropical SST anomalies are mainly driven by the extratropical atmosphere, the model simulations show that SST anomalies associated with PC2 have a feedback on the PNA and the WP. Apart from the variations in Pacific SST anomalies, there are many other factors that may have impacts on the stratospheric polar vortex and SSWs in winter. Some previous studies have revealed that the stratospheric polar vortex is impacted to a large extent by the lower stratospheric equatorial QBO (Holton and Tan 1980; Gray 2003; Naoe and Shibata 2010; White et al. 2015). Another important force contributing to the atmospheric decadal variabilities is the 11-year solar cycle (SC). There is a significant SC signal in the winter in the northern polar stratosphere, as reported by many previous studies (e.g., Labitzke et al. 2006; Ito et al. 2009). In addition, PC1 and PC2 involve different processes at different time scales such as the modes of the Kuroshio-Oyashio extension region. These processes can influence PC1 and PC2 and simultaneously affect atmospheric variables (Di Lorenzo et al. 2010; Newman et al. 2016). Further works are necessary to clarify the potential impacts of all these factors on the decadal variations in SSWs.

**Acknowledgements** We are grateful to the groups and agencies that provided the datasets analyzed in this study. This work is supported by the National Natural Science Foundation of China (41225018, 41575038 and 41630421).

## References

Andrews DG, Holton JR, Leovy CB (1987) Middle atmosphere dynamics. Academic press, San Diego

Baldwin MP, Dunkerton TJ (2001) Stratospheric harbingers of anomalous weather regimes. Science 294:581–584

Bell CJ, Gray LJ, Charlton-Perez AJ, Joshi MM, Scaife AA (2009) Stratospheric communication of El Niño teleconnections to European winter. J Clim 22:4083–4096

Bond N, Overland J, Spillane M, Stabeno P (2003) Recent shifts in the state of the North Pacific. Geophys Res Lett 30:2183. doi:10.1029/2003GL018597

Bretherton CS, Widmann M, Dymnikov VP, Wallace JM, Bladé I (1999) The effective number of spatial degrees of freedom of a time-varying field. J Clim 12:1990–2009

Brönnimann S (2007) Impact of El Niño–southern oscillation on European climate. Rev Geophys 45:RG3003. doi:10.1029/2006RG000199

Butler AH, Seidel DJ, Hardiman SC, Butchart N, Birner T, Match A (2015) Defining sudden stratospheric warmings. Bull Am Meteor Soc 96:1913–1928. doi:10.1175/BAMS-D-13-00173.1

Calvo N, Garcia RR, Randel WJ, Marsh DR (2010) Dynamical mechanism for the increase in tropical upwelling in the lowermost tropical stratosphere during warm ENSO events. J Atmos Sci 67:2331–2340

Charlton AJ, Polvani LM (2007) A new look at stratospheric sudden warmings. Part I: Climatology and modeling benchmarks. J Clim 20:449–469

Chhak KC, Di Lorenzo E, Schneider N, Cummins PF (2009) Forcing of low-frequency ocean variability in the Northeast Pacific*. J Clim 22:1255–1276

Garcia RR, Marsh DR, Kinnison DE, Boville BA, Sassi F (2007) Simulation of secular trends in the middle atmosphere, 1950–2003. J Geophys Res Atmos 112:D09301. doi:10.1029/2006JD007485.

Di Lorenzo E, Schneider N, Cobb K, Franks P, Chhak K, Miller A, McWilliams J, Bograd S, Arango H, Curchitser E (2008) North Pacific Gyre oscillation links ocean climate and ecosystem change. Geophys Res Lett 35:L08607. doi:10.1029/2007GL032838

Di Lorenzo E, Cobb KM, Furtado JC, Schneider N, Anderson BT, Bracco A, Alexander MA, Vimont DJ (2010) Central Pacific El Nino and decadal climate change in the North Pacific Ocean. Nat Geosci 3:762–765

Ding R, Li J, Tseng Y, Sun C, Guo Y (2015) The Victoria mode in the North Pacific linking extratropical sea level pressure variations to ENSO. J Geophys Res Atmos 120(1):27–45

Furtado JC, Di Lorenzo E, Schneider N, Bond NA (2011) North Pacific decadal variability and climate change in the IPCC AR4 models. J Clim 24:3049–3067

Garfinkel CI, Hartmann DL (2008) Different ENSO teleconnections and their effects on the stratospheric polar vortex. J Geophys Res Atmos 113:D18114. doi:10.1029/2008JD009920
Gray LJ (2003) The influence of the equatorial upper stratosphere on stratospheric sudden warmings. Geophys Res Lett 30:1166. doi:10.1029/2002GL016430
Holton JR (1976) A semi-spectral numerical model for wave-mean flow interactions in the stratosphere: application to sudden stratospheric warmings. J Atmos Sci 33:1639–1649
Holton JR, Tan HC (1980) The influence of the equatorial quasi-biennial oscillation on the global circulation at 50 mb. J Atmos Sci 37:2200–2208
Horel JD, Wallace JM (1981) Planetary-scale atmospheric phenomena associated with the Southern Oscillation. Mon Wea Rev 109:813–829
Hu Y, Pan L (2009) Arctic stratospheric winter warming forced by observed SSTs. Geophys Res Lett 36(11). doi:10.1029/2009GL037832
Hu D, Tian W, Xie F, Shu J, Dhomse S (2014) Effects of meridional sea surface temperature gradients on the stratospheric temperature and circulation. Adv Atmos Sci 31:888–900. doi:10.1007/s00376-013-3152-6
Hurwitz MM, Newman PA, Garfinkel CI (2011) The Arctic vortex in March 2011: a dynamical perspective. Atmos Chem Phys 11:11447–11453. doi:10.5194/acp-11-11447-2011
Hurwitz MM, Newman PA, Garfinkel CI (2012) On the influence of North Pacific sea surface temperature on the Arctic winter climate. J Geophys Res Atmos 117:D19110. doi:10.1029/2012JD017819
Ito K, Naito Y, Yoden S (2009) Combined effects of QBO and 11-year solar cycle on the winter hemisphere in a stratosphere-troposphere coupled system. Geophys Res Lett 36:L11804. doi:10.1029/2008GL037117
Jadin EA, Wei K, Zyulyaeva YA, Chen W, Wang L (2010) Stratospheric wave activity and the Pacific Decadal Oscillation. J Atmos Sol-Terr Phy 72:1163–1170. doi:10.1016/j.jastp.2010.07.009
Kren AC, Marsh DR, Smith AK, Pilewskie P (2016) Wintertime northern hemisphere response in the stratosphere to the pacific decadal oscillation using the whole atmosphere community climate model. J Climate 29:1031–1049 doi. doi:10.1175/JCLI-D-15-0176.1
Krüger K, Naujokat B, Labitzke K (2005) The unusual midwinter warming in the Southern Hemisphere stratosphere 2002: a comparison to Northern Hemisphere phenomena. J Atmos Sci 62:603–613
Kushnir Y, Robinson WA, Blade I, Hall N M J, Peng S, Sutton R (2002) Atmospheric GCM response to extratropical SST anomalies: synthesis and evaluation. J Clim 15(16):2233–2256
Kwon YO, Deser C (2007) North pacific decadal variability in the community climate system model version 2. J Clim 20(11):2416–2433
Labitzke K, Kunzel M, Broennimann S (2006) Sunspots, the QBO and the stratosphere in the North Polar Region—20 years later. Meteorol Z 15:355–363
Li Y, Tian W (2017) Different impact of central pacific and eastern Pacific El Niño on SSW duration. Adv Atmos Sci 34(6):771–782. doi:10.1007/s00376-017-6286-0
Li Y, Li J, Feng J (2012) A teleconnection between the reduction of rainfall in Southwest Western Australia and North China. J Clim 25:8444–8461
Mantua NJ, Hare SR (2002) The Pacific decadal oscillation. J Oceanogr 58(1):35–44
Mantua NJ, Hare SR, Zhang Y, Wallace JM, Francis RC (1997) A Pacific interdecadal climate oscillation with impacts on salmon production. Bull Am Meteor Soc 78:1069–1079
Martius O, Polvani LM, Davies HC (2009) Blocking precursors to stratospheric sudden warming events. Geophys Res Lett 36:L14806. doi:10.1029/2009GL038776
Matsuno T (1970) Vertical propagation of stationary planetary waves in the winter Northern Hemisphere. J Atmos Sci 27:871–883
Matsuno T (1971) A dynamical model of the stratospheric sudden warming. J Atmos Sci 28:1479–1494
Mitchell DM, Gray LJ, Anstey J, Baldwin MP, Charlton-Perez AJ (2013) The influence of stratospheric vortex displacements and splits on surface climate. J Climate 26:2668–2682. doi:10.1175/jcli-d-12-00030.1
Nakamura H, Lin G, Yamagata T (1997) Decadal climate variability in the North Pacific during the recent decades. Bull Am Meteor Soc 78:2215–2225
Naoe H, Shibata K (2010) Equatorial quasi-biennial oscillation influence on northern winter extratropical circulation. J Geophys Res Atmos 115:D19102. doi:10.1029/2009JD012952
Newman M, Compo GP, Alexander MA (2003) ENSO-forced variability of the pacific decadal oscillation. J Clim 16:3853–3857. doi:10.1175/1520-0442(2003)016<3853:EVOTPD>2.0.CO;2
Newman M, Alexander MA, Ault TR, Cobb KM, Deser C, Di Lorenzo E, Mantua NJ, Miller AJ, Minobe S, Nakamura H (2016) The Pacific decadal oscillation, revisited. J Clim 29:4399–4427. doi:10.1175/JCLI-D-15-0508.1
Nigam S (2003) Teleconnections. Encyclopedia of atmospheric sciences, Holton JR, Pyle JA, Curry JA (eds) Elsevier, pp 2243–2269
Nishii K, Nakamura H, Orsolini YJ (2010) Cooling of the wintertime Arctic stratosphere induced by the western Pacific teleconnection pattern. Geophys Res Lett 37:L13805. doi:10.1029/2010GL043551
O'Neill A (2003) Stratospheric sudden warmings. Encyclopedia of atmospheric sciences. In: Holton JR, Pyle JA, Curry JA (eds) Elsevier, pp 1342–1353
Pawson S, Naujokat B (1999) The cold winters of the middle 1990s in the northern lower stratosphere. J Geophys Res Atmos 104:14209–14222
Pierce DW, Barnett TP, Schneider N, Saravanan R, Dommenget D, Latif M (2001) The role of ocean dynamics in producing decadal climate variability in the North Pacific. Clim Dyn 18:51–70
Quiroz RS (1986) The association of stratospheric warmings with tropospheric blocking. J Geophys Res 91:5277–5285
Rayner N, Parker DE, Horton E, Folland C, Alexander L, Rowell D, Kent E, Kaplan A (2003) Global analyses of sea surface temperature, sea ice, and night marine air temperature since the late nineteenth century. J Geophys Res Atmos 108:4407. doi:10.1029/2002JD002670
Reichler T, Kim J, Manzini E, Kröger J (2012) A stratospheric connection to Atlantic climate variability. Nat Geosci 5:783–787
Ren RC, Cai M, Xiang C, Wu G (2011) Observational evidence of the delayed response of stratospheric polar vortex variability to ENSO SST anomalies. Clim Dyn 38:1345–1358. doi:10.1007/s00382-011-1137-7
Taguchi M, Hartmann DL (2006) Increased occurrence of stratospheric sudden warmings during El Nino as simulated by WACCM. J Clim 19:324–332
Wallace JM, Gutzler DS (1981) Teleconnections in the geopotential height field during the Northern Hemisphere winter. Mon Wea Rev 109:784–812
Wang L, Chen W (2010) Downward Arctic Oscillation signal associated with moderate weak stratospheric polar vortex and the cold December 2009. Geophys Res Lett 37:L09707. doi:10.1029/2010GL042659
Waugh DW, Polvani LM (2010) Stratospheric polar vortices. In: Polvani LM, Sobel AH, Waugh DW (eds) The stratosphere: dynamics, transport and chemistry. American Geophysical Union, Washington, DC
White IP, Lu H, Mitchell NJ, Phillips T (2015) Dynamical response to the QBO in the Northern Winter stratosphere: signatures in

wave forcing and Eddy fluxes of potential vorticity. J Atmos Sci 72:4487–4507. doi:10.1175/JAS-D-14-0358.1

Woo S-H, Sung M-K, Son S-W, Kug J-S (2015) Connection between weak stratospheric vortex events and the Pacific Decadal Oscillation. Clim Dyn 45:3481–3492

Woollings T, Charlton-Perez A, Ineson S, Marshall AG, Masato G (2010) Associations between stratospheric variability and tropospheric blocking. J Geophys Res Atmos 115:D06108. doi:10.1029/2009JD012742

Wu L, Liu Z (2005) North Atlantic decadal variability: air-sea coupling, oceanic memory, and potential northern hemisphere resonance. J Clim 18(2):331–349

Zhang J, Tian W, Wang Z, Xie F, Wang F (2015) The influence of ENSO on Northern Midlatitude ozone during the winter to spring transition. J Clim 28:4774–4793